Visualizing Poincaré Maps Together With the Underlying Flow

Helwig Löffelmann, Thomas Kučera, and Eduard Gröller *

Institute of Computer Graphics, Vienna University of Technology,
Karlsplatz 13/186/2, A-1040 Wien, Austria **

Abstract. We present a set of advanced techniques for the visualization of 2D Poincaré maps. Since 2D Poincaré maps are a mathematical abstraction of periodic or quasi-periodic 3D flows, we propose to embed the 2D visualization with standard 3D techniques to improve the understanding of the Poincaré maps. Methods to enhance the representation of the relation $x \leftrightarrow P(x)$, e.g., the use of spot noise, are presented as well as techniques to visualize the repeated application of P, e.g., the approximation of P as a warp function. It is shown that animation can be very useful to further improve the visualization. For example, the animation of the construction of Poincaré map P is a very intuitive visualization. During the paper we present a set of examples which demonstrate the usefulness of our techniques.

Keywords: visualization, dynamical systems, Poincaré maps

1 Introduction

Poincaré sections are an important tool for the investigation of dynamical systems in theory as well as in applications. They are used for models (usually in 3D) that exhibit periodic or quasi-periodic behavior. In addition to mathematical descriptions—there is a lot of theory about dynamical systems [3,4,7,16]—periodic or quasi-periodic dynamical systems can be found in many fields, e.g., in physics, chemistry, biology, ecology. Especially chaotic systems are often examined by the use of Poincaré sections [13,14,16].

Roughly speaking a 2D Poincaré section through a periodic 3D flow is a planar cross-section transverse to the flow such that a periodic orbit intersects it at its center. The corresponding Poincaré map is defined as a map correlating consecutive intersections of flow trajectories with the Poincaré section. The Poincaré map is a discrete dynamical system of one dimension less than the continuous flow which it is constructed from. Since many of the most important flow properties are inherited by the Poincaré map and its analysis is usually more simple due to its reduced dimensionality, it is often used for analysis instead of the 3D flow. See Sect. 2 for a little bit more detailed discussion of some basics on Poincaré sections and Poincaré maps.

* Email: { helwig | tkucera | groeller } @cg.tuwien.ac.at

** URL: http://www.cg.tuwien.ac.at/home/

Since their introduction to dynamical system analysis by Henri Poincaré in 1899 [12] the visual representation of Poincaré maps has been always a very important part of this research technique. Hand-drawn sketches of the Poincaré map were used for a long time to guide or illustrate the mathematical analysis [1]. Due to the ability of integrating a dynamical system numerically by the use of a computer, visualization techniques that are based on the numerical approximation of the Poincaré map have become popular [11,14]. There are a number of programs that calculate Poincaré maps [6]. See Sect. 3 for a brief review of previous work in this field.

Most visualization techniques for Poincaré maps suffer from rather severe limitations. One problem is, that with the use of 2D visualization techniques the context of the 3D flow is lost. Certain features, e.g, the number of windings of a Möbius band, can not be derived from the 2D Poincaré map alone. Another problem with these techniques is that the temporal correlation between points of the Poincaré map is not encoded within the 2D image. Most limitations of the 2D techniques in this field are usually not due to a weakness of the software or method, but rather due to an inherent difficulty with dimension reduction approaches.

We therefore propose a set of advances within this rather untouched field of visualization. First, we suggest to adapt some well-known visualization techniques as, e.g., spot noise, to Poincaré maps to improve the visual representation of the 2D map. See Sect. 4 for a discussion of these ideas. Furthermore we present an embedding of these techniques within a 3D visualization of the underlying flow. This approach allows to significantly reduce some limitations of previously known techniques. Please refer to Sect. 5 for a description of this approach. Our ideas are implemented within DynSys3D [9], an experimental workbench for the development of advanced visualization techniques in the field of dynamical systems. The capabilities of the implementation are illustrated with some examples in Sect. 7. We draw some conclusions in Sect. 8 and give ideas for future work.

2 About Poincaré Maps

A *Poincaré section* is used to construct a $(n-1)$-dimensional discrete dynamical system, i.e., a *Poincaré map*, of a continuous flow given in n dimensions. This reduced system of $(n-1)$ dimensions inherits many properties, e.g., periodicity or quasi-periodicity, of the original system. We will concentrate in the following on the important case of n being equal to three.

Poincaré maps are used to investigate periodic or quasi-periodic dynamical systems. Often these systems exhibit a periodic cycle or a chaotic attractor. A Poincaré section $\mathcal{S}$ is now assumed to be a part of a plane, which is placed within the 3D phase space of the continuous dynamical system such that either the periodic orbit or the chaotic attractor intersects

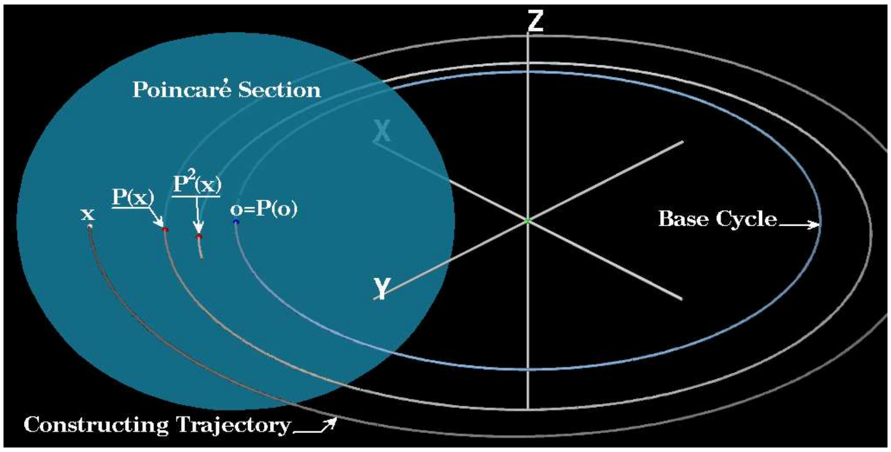

Fig. 1. An illustration of the Poincaré map definition (cf. color plate 1)

the Poincaré section. The Poincaré map is now defined as a discrete function $P : \mathcal{S} \to \mathcal{S}$, which associates consecutive intersections of a trajectory of the 3D flow with $\mathcal{S}$ (see Fig. 1).

There are some important relations between a 3D flow and the corresponding Poincaré map: Cycles $\mathcal{C}$ of the 3D system which intersect the Poincaré section $\mathcal{S}$ in q points ($q \geq 1$) are related to periodic points $o = \mathcal{C} \cap \mathcal{S} = P^q(o)$ of Poincaré map P, i.e., o is a fixed point of the map P^q. Furthermore stability characteristics of the cycle are inherited by the fixed point: stable, unstable, or saddle cycles result in stable, unstable, or saddle nodes, respectively. Therefore many characteristics of periodic or quasi-periodic dynamical systems can be derived from the corresponding Poincaré map.

3 Previous and Related Work

Visualization techniques have been used for the illustration of Poincaré maps since they were introduced by Henry Poincaré. Most of these imaging methods are 2D or 1D plots that are calculated by numerically integrating the underlying flow.

In addition to these traditional 2D plots a few more general techniques can be found in the literature. Hand-drawn images in a book by Abraham and Shaw [1] demonstrate that a combination of the Poincaré section and the underlying 3D flow within within a single image convey a better understanding of the underlying flow characteristics. The book by Abraham and Shaw is in effect quite an inspirational source. We think that a number of artistic techniques used for the hand-drawn images in the book are well-suited for computer-supported visualization techniques. Streamarrows [10] are another approach to automate techniques presented in this book.

4 Visualizing Poincaré Maps

The contribution of this paper can be divided into two parts. First, we suggest a set of advanced visualization techniques directly applicable to 2D Poincaré maps. We describe these techniques in subsections 4.1 and 4.2. Secondly, we demonstrate how an embedding of our techniques within a 3D flow visualization improves the expressiveness of images and animations. See Sect. 5 for a discussion of this part of our work.

In this section we focus on a 2D Poincaré section $\mathcal{S}$ and how the mathematical method of analysis by the use of Poincaré map P can be supported by visualization. Different aspects of $\mathcal{S}$ or P are of interest and might therefore be visualized. The transformation of $\mathcal{S}$ under the application of P is certainly the most important issue to visualize (see Sect. 4.1). Additionally the repeated application of the Poincaré map, namely P^n, is also often investigated. This is done, for example, when the asymptotical behavior of the map is studied (see Sect. 4.2).

4.1 Visualizing Poincaré Map *P*

As Poincaré map P maps points x onto $P(x)$ both lying in $\mathcal{S}$, a visualization based on (directed) strokes connecting x and $P(x)$ has been done. We implemented a module named FLOW that generates a set of arrows on the Poincaré section, which all start in some point x_i and end in correlated $P(x_i)$. See Fig. 2 for a visualization of a non-linear saddle cycle where this technique was used. $\mathcal{S}$ is represented as a semi-transparent disk. A set of light-grey arrows is placed on $\mathcal{S}$ to visualize P^1. Sequences of consecutive applications of P are visualized by the use of small red spheres, representing $\{P^j(x_i)\,|\,j \geq 0\}$, whereby the sphere depicting $P^0(x_i)$ is colored differently from the others. The visualization of sequence $\{P^j(x_i)\,|\,j \geq 0\}$, which starts near the origin of phase space, is furthermore enhanced by combining it with a visualization of the constructing flow trajectory.

We also adapted spot noise [15] to Poincaré maps. We place elliptic spots onto $\mathcal{S}$ such that the focal points of the ellipses coincide with x_i and $P(x_i)$, respectively. This choice is due to the fact that no directional information should be encoded, when $P(x_i) = x_i$. In this case both focal points coincide and the elliptic spot degenerates to a circle. Images rendered with this method are well suited to visualize the entirety of $P(\mathcal{S})$ within one still image. See Fig. 3 for a visualization of a non-hyperbolic saddle cycle (3 stable and 3 unstable manifolds), where spot noise was used for visualization.

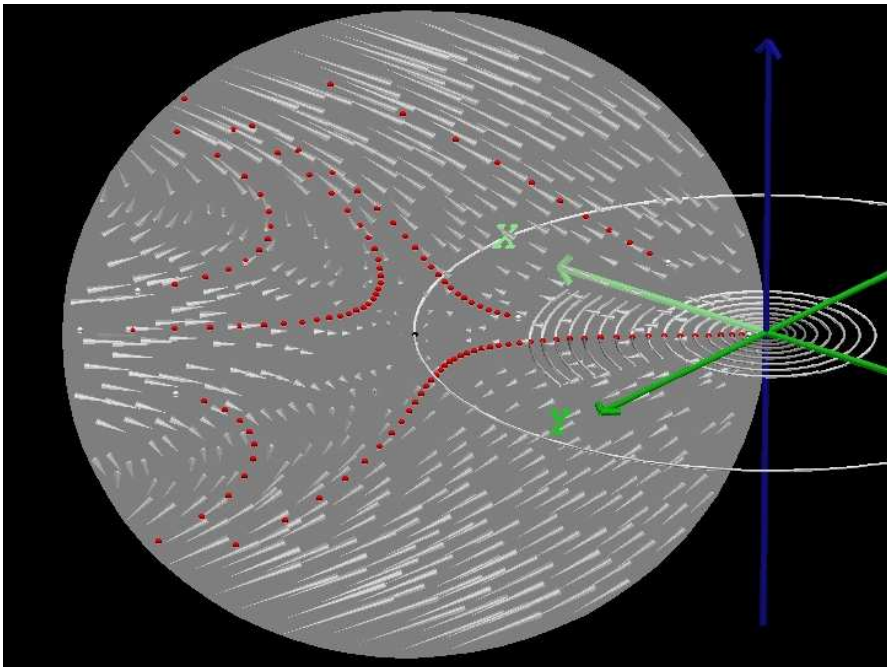

Fig. 2. Visualizing a non-linear saddle cycle (see also color plate 3)

Similar as in Fig. 2 white and red spheres are used to visualize certain sequences $\{P^j(x_i) \,|\, j \geq 0\}$.

The results of the previous techniques are embedded into a 3D visualization of the underlying flow. We therefore represent Poincaré section $\mathcal{S}$ as a semi-transparent disk placed within the flow and realized the arrows and spot noise as a texture of this disk (cf. Figs. 2 & 3). Semi-transparency was used for the map to allow the viewer to see through. This improves the understanding of the context of map P.

4.2 Visualizing the Repeated Application P^n

There are several reasons to investigate the repeated application of Poincaré map P, i.e., P^n. Probably the most important one is the analysis of the asymptotic behavior induced by the (iterated) Poincaré map. Periodic systems near a cycle can exhibit different asymptotical behavior, e.g., convergence or divergence with respect to the cycle. This aspect is due to different possible cycle characteristics, namely stable, saddle, or unstable behavior. A stable cycle attracts near trajectories, whereas unstable and saddle cycles repel near trajectories. A saddle cycle $\mathcal{C}$ separates its Poincaré section $\mathcal{S}$ into regions of attraction and such of repulsion. Almost all trajectories

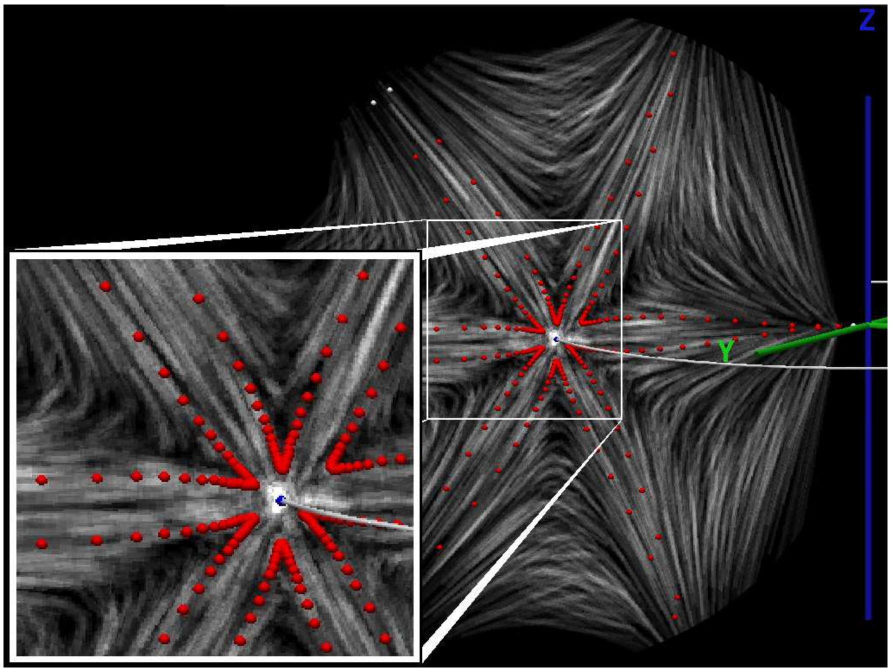

Fig. 3. Visualizing a non-hyperbolic saddle cycle (see color plate 4)

near $o = P(o)$ emerge into the repelling parts of $\mathcal{S}$ and thus are finally repelled from $\mathcal{C}$. Figures 2 and 3 show two Poincaré maps of different saddle cycles.

We implemented a module TRAJECTORY which produces a visualization of the set $\{P^j(x_i) \,|\, j \geq 0\}$ by generating a sphere for each $P^j(x_i)$. See, e.g, the small red spheres in Figs. 2 & 3 for examples where this module was used. The sphere representing $P^0(x_i) = x_i$ is colored differently from all the others such that the origin of a sequence can be identified (cf. Fig. 3).

Sometimes P^q, $q > 1$ is more interesting to investigate than P. This is the case, for example, when base cycle $\mathcal{C}$ itself pierces $\mathcal{S}$ q times during one complete loop (see Fig. 4). In the given example $\mathcal{C}$ intersects $\mathcal{S}$ two more times before it returns to the initial intersection point and thus closes the cycle. The behavior of trajectories $\mathcal{T}$ near $\mathcal{C}$ are better described by one arbitrary $x \in \mathcal{T} \cap \mathcal{S}$ & $P^3(x)$ rather than x & $P(x)$. In fact any pair $(P^j(x), P^{j+q}(x))$, $0 \leq j < q$, can be chosen for this improved analysis.

The user can change the default value of q, i.e., 1, such that all the previously discussed visualization techniques, e.g., spot noise, are adapted to this new parameter setting. Moreover we allow the user to specify that only those intersections $y = \mathcal{T} \cap \mathcal{S}$ are considered where $f(y) \cdot f(\mathcal{C} \cap \mathcal{S}) > 0$ (f being the underlying 3D flow). Only those points on trajectory $\mathcal{T}$ are of

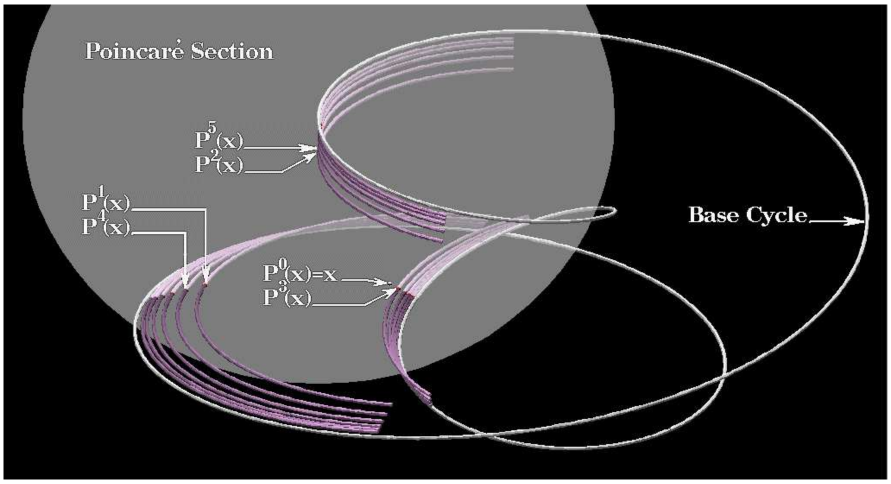

Fig. 4. Visualizing why P^q is sometimes more expressive than P

interest where $\mathcal{T}$ crosses the Poincaré section with the same orientation. This means that $\mathcal{T}$ crosses $\mathcal{S}$ in both cases either in front-to-back or back-to-front orientation. In Fig. 5 the left image was rendered with $q = 1$ and the right one with $q = 3$. In this case the base cycle pierces $\mathcal{S}$ three times during one complete loop.

Although there are still some artifacts in the right image which are due to the limited size of $\mathcal{S}$, it is more expressive than the left one. The egg-shaped intersection of an invariant torus (containing the base cycle) and Poincaré section $\mathcal{S}$ can be clearly seen as dark line around the center of this image. Furthermore the unstable cycle within this torus cross-section can be distinguished as a fixed point of the Poincaré map P. The radial repulsion

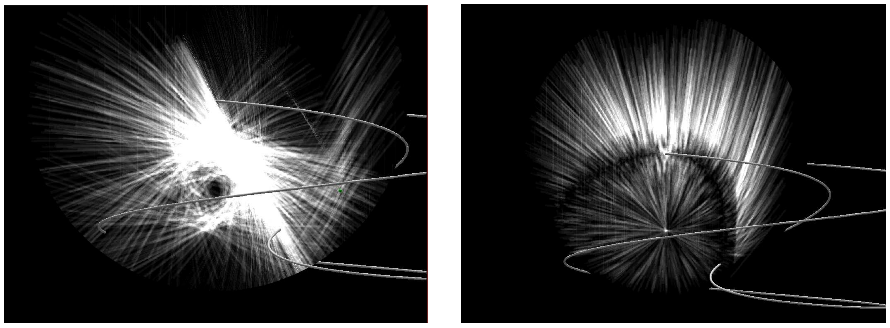

(a) (b)

Fig. 5. Visualizing $\{(x_i, P(x_i))\}$ (a) vs. $\{(x_i, P^3(x_i))\}$ (b)

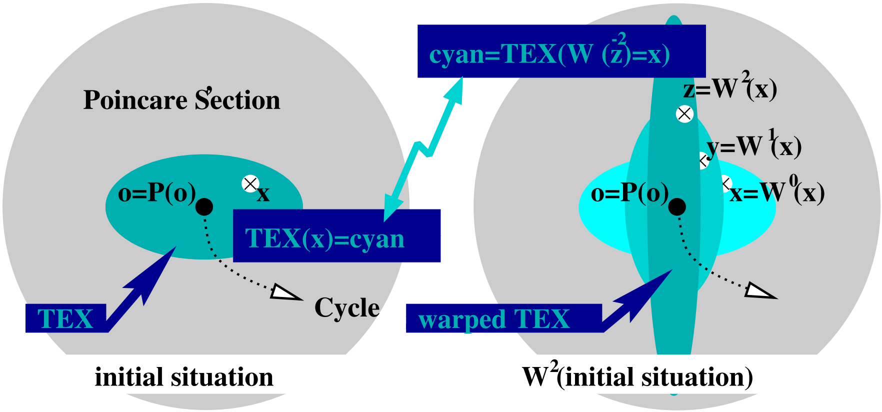

Fig. 6. Evaluating the initial texture after two applications of W (cf. color plate 5)

away from this fixed point towards the torus is well represented by the star like spot noise texture.

The visualization of P^n, $n > 1$, is more difficult than visualizing P itself. A technique we investigated for the representation of P^n, n increasing, is image warping [5]. We implemented a module Warp that approximates P by a warp function W on the basis of $\mathcal{L}$ and $P(\mathcal{L})$ where $\mathcal{L}$ can be chosen to be either a jittered or regular set of line segments spread over $\mathcal{S}$. Warp loads an initial texture TEX onto $\mathcal{S}$ and then applies W n times, where n is specified via a parameter of Warp. The resulting texture $TEX \circ W^{-n}$ (cf. Fig. 6) placed on $\mathcal{S}$ gives a good impression of the main characteristics of P^n. See Fig. 9 for an image series rendered using this technique. The reason why we approximate Poincaré map P by the use of a warping function instead of using P directly for the transformation of the texture is that P is usually rather costly to compute. Warp function Warp on the other hand is capable of approximating P quite good if P is sufficiently smooth ans warping parameters are chosen apropriatly. At least an idea of P^n is gained using this technique.

5 Embedding the Visualization of Poincaré Maps within the 3D Flow

The simultaneous visualization of a Poincaré map and the underlying flow allows to overcome some limitations of 2D visualization techniques of Poincaré maps. Flow characteristics which cannot be derived from 2D Poincaré maps alone as, e.g, the relation between consecutive intersections, can be made visible and thus enrich the capabilities of this visualization technique.

A Poincaré section $\mathcal{S}$ is represented as a circular patch that is rendered semi-transparently. Therefore visualization icons before as well as behind $\mathcal{S}$ are visible. Our current implementation is based on the existence of a base cycle $\mathcal{C}$ within the 3D flow. Cycle $\mathcal{C}$ defines the center of Poincaré section $\mathcal{S}$. The cycle $\mathcal{C}$ is rendered as an opaque tube through 3D phase space together with a sphere at $\mathcal{C} \cap \mathcal{S}$ where the base cycle intersects the Poincaré section. See Fig. 2 or 3 for an image where $\mathcal{S}$, $\mathcal{C}$, and the intersection $\mathcal{C} \cap \mathcal{S}$ can be easily detected.

The module which generates this Poincaré map visualization takes care that initially a useful view point is chosen. $\mathcal{S}$ is viewed under an angle which is little bit less than $\pi/2$ so that both the Poincaré map and the intersecting base cycle are easily recognizable (see Fig. 2). We also found it very useful to provide a relative placement capability such that the user can move the Poincaré section easily around the base cycle $\mathcal{C}$. The actual position of the map on the cycle is specified by a value between 0 and 1.

Additionally we suggest some more elaborated 3D extensions to Poincaré map visualization. Module TRAJECTORY, for example, generates either the entire trajectory which constructs the sequence $\Omega = \{P^j(x) \,|\, j \geq 0\}$, only short parts of this trajectory in the vicinity of $\mathcal{S}$, or just the spheres representing the consecutive intersections.

Drawing the entire trajectory that generates sequence Ω, for example, helps to relate consecutive points on $\mathcal{S}$ mentally (cf. Figs. 1 & 4). Long trajectories, however, may clutter the image.

Using only short parts of the trajectory near $\mathcal{S}$ avoids the problem of visual clutter (see Fig. 7). Assume a periodic 3D system which exhibits some high frequency oscillation parallel to the rotational axis of the flow (see Fig. 7, left image). If the frequency (measured in oscillations per one total revolution of the carrying periodic system around the rotational axis of the flow) is an integer number, the resulting Poincaré map is not affected by this oscillation at all. Results are the same as for a system without the modulated frequency. Compare left and right image in Fig. 7.

Both images in Fig. 7 are generated with techniques already discussed previously in this paper. Spot noise is used to represent the entirety of P, whereas white and red spheres are used to visualize three sequences $\{P^j(x_i) \,|\, j \geq 0\}$. The one sequence starting near the origin of phase space is enhanced by short parts of the constructing flow trajectory. This enhancement is necessary to visualize the differences between both systems.

Another technique for the investigation of Poincaré maps is realized as module SEEDLINE. By parameters r, ϕ, and $dist$ a line segment $\mathcal{Y}$ of length $2 \cdot \mathrm{R}$ is specified within $\mathcal{S}$ that is perpendicular to the vector connecting $\mathcal{C} \cap \mathcal{S}$ and the mid-point of $\mathcal{Y}$. The length of this vector is specified by parameter $dist$. Parameters ϕ and r are the polar coordinates of one endpoint of this line segment with respect to its mid-point. SEEDLINE can be

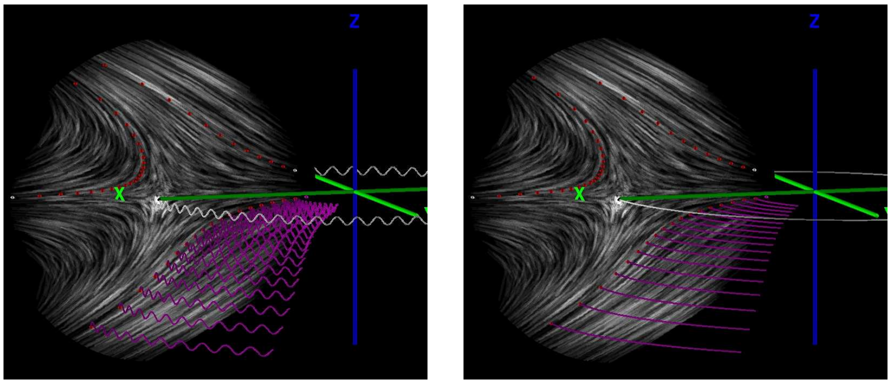

Fig. 7. Visualizing supplementary information in 3D (cf. color plate 7)

used to generate a streamsurface [8] or a rag of streamlines alternatively (see Fig. 8). In addition to the supplementary streamsurface, the flow trajectory, which constructs a certain sequence of consecutive applications of P, was visualized by the use of a green tube. Other techniques discussed previously in this paper have been used for visualizing Poincaré section $\mathcal{S}$.

6 Animation Aspects

Animation is a powerful approach to increase the dimensionality of visualization results. We found the following parameters of our modules suitable to be animated:

TRAJECTORY parameters *no* and *len* – Module TRAJECTORY generates a sequence Ω of consecutive intersections of trajectory $\mathcal{T}$ and Poincaré section $\mathcal{S}$, i.e., $\Omega = \mathcal{T} \cap \mathcal{S}$. Parameter *no* specifies how many intersections should be calculated. *len* can be used to control $|\Omega|$ via the spatial length of $\mathcal{T}$.
Animating one of these two parameters, the construction of the Poincaré map P can be visualized. Furthermore the asymptotical behavior of $P^n(x)$, $n \to \infty$ can be investigated. This specific application of animation is capable of representing the *inherent* nature of Poincaré map P.

TRAJECTORY parameters r and ϕ – Another pair of TRAJECTORY parameters, which is very well suited for animation, is (ϕ, r). It encodes the initial condition x of solution $\mathcal{T}(x)$ in polar coordinates with respect to some arbitrary local coordinate system on $\mathcal{S}$. In other words (ϕ, r) specifies the starting point of sequence $P^j(x)$, $j \geq 0$.
Animating these two parameters allows to investigate the development of arbitrary curves $\mathcal{Q}$ within $\mathcal{S}$. Such a curve $\mathcal{Q} = (\mathcal{Q}_\phi(s), \mathcal{Q}_r(s))$ should

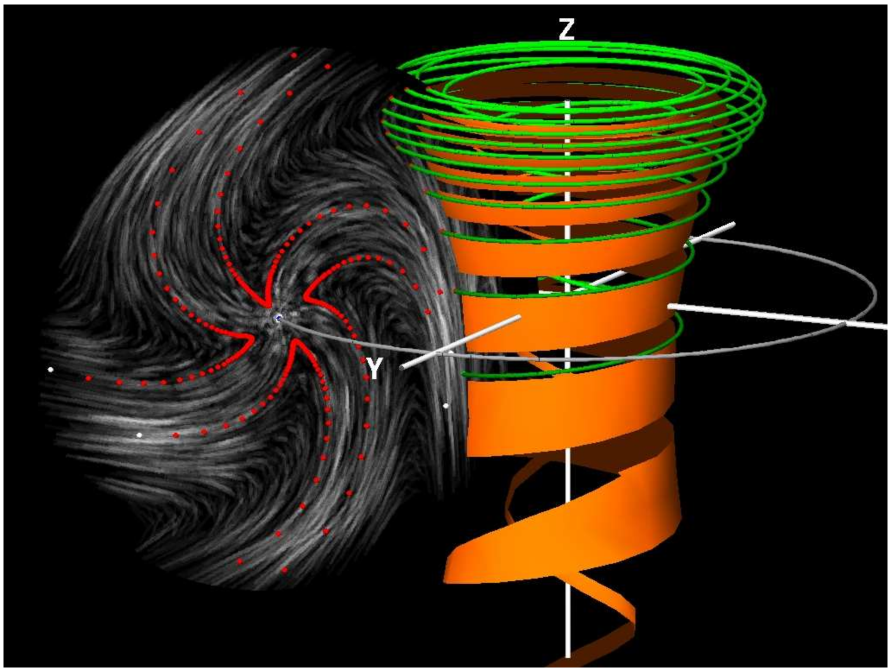

Fig. 8. Enhancing the 2D Poincaré map visualization by the use of 3D flow visualization icons (see also color plate 2)

be given as a parameterized subset of $\mathcal{S}$ with s as the parameter. Given such a curve $\mathcal{Q}$, parameter s can be animated: The module TRAJECTORY takes $x(s) = (\mathcal{Q}_\phi(s), \mathcal{Q}_r(s))$ as an initial condition for the generation of $\{P^j(x(s)) \,|\, j \geq 0\}$. Initial condition $x(s)$ moves along curve $\mathcal{Q}$, and simultaneously its long-term future $\{P^j(x(s)) \,|\, j \geq 0\}$ is visualized.

WARP parameter n – The animation of WARP parameter n (number of applications) improves the expressiveness of the image warping approach. A sequence of images with consecutive applications of warping function W shows efficiently the overall behavior of P^n, $n \to \infty$. Refer to Fig. 9 for three images resulting from consecutive applications of the warping function W.

7 Implementation Issues

All the visualization techniques proposed in this paper have been implemented within DynSys3D [9], which is a flexible development workbench for advanced visualization techniques of three-dimensional dynamical systems. DynSys3D itself is based on AVS [2], which is a general purpose visualization

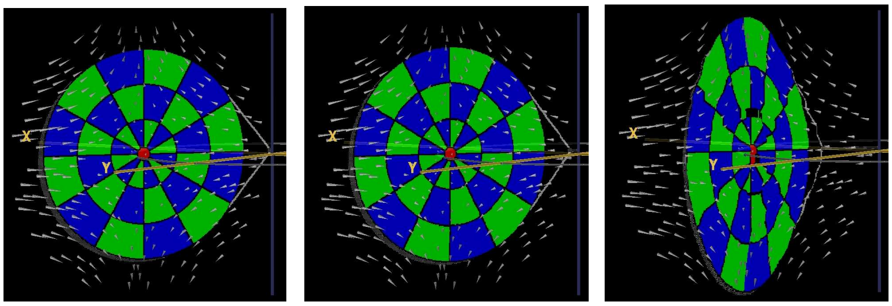

Fig. 9. Images resulting from one, two, and eleven applications of warp function W, i.e., $W(\mathcal{S})$, $W^2(\mathcal{S})$, and $W^{11}(\mathcal{S})$ (color plate 6)

system. A main feature of DynSys3D is the treatment of *dynamical system*, *numerical integrator*, and *visualization technique* as separate components. Thereby it is very easy to extend this system by a new visualization technique or an additional dynamical system. Dynamical systems are specified analytically within DynSys3D.

A Poincaré map is realized as a new *visualization technique* named MAP. It provides the core functionality of all the techniques presented here. Additionally modules TRAJECTORY, FLOW, SEEDLINE, and WARP have been implemented as separate modules which are connected to basis module MAP in case one of the previously described visualization mappings should be instantiated. These modules allow a flexible composition of an arbitrary number of visualization mappings.

Additionally we investigated a set of dynamical systems to test our techniques. We constructed five simple systems that exhibit most of the characteristics usually obtained in periodic systems. See the Appendix for a brief note on the construction of these periodic dynamical systems.

8 Conclusions

The use of Poincaré sections for the investigation and analysis of periodic or quasi-periodic dynamical systems has become an established technique quite a long time ago. The investigation of, e.g., chaotic dynamical systems together with informative pictures of Poincaré maps strengthened the importance of this technique. The vast majority of visualization techniques for Poincaré maps are based on 2D plots of 3D systems.

We propose several advances to this field in our paper. On the one hand we suggest some improvements of the planar visualization of Poincaré maps. We place arrow-like icons on the Poincaré section that connect x and $P(x)$.

Thereby the dynamics induced by the Poincaré map is visualized. Alternatively a technique similar to Wijk's spot noise can be used to visualize the entirety of P. The visualization of a repeated application of P is also very important. We use spheres to depict series $\{P^j(x) \mid j \geq 0\}$.

In addition to the enhanced planar visualizations of Poincaré map P we discussed how an embedding of these techniques within the underlying dynamical system can be done. Drawing the entire trajectory which constructs series $\{P^j(x) \mid j \geq 0\}$ or just parts of it can give important information on the relation between points of the Poincaré map. Additional information about the characteristics of the underlying flow as, e.g., the number of windings of a Möbius band, is visualized, which cannot be derived from planar visualization. Using streamsurfaces to enhance the visualization of the underlying flow improves the representation of the combined flow and Poincaré map.

Together with both approaches animation techniques must be revisited carefully. Meaningful applications can be found, for example, the consecutive construction of the Poincaré map by animating the underlying flow. Animation can be used as an additional dimension of visualization and thus provides additional possibilities. For example, the visualization of the entirety of repeated application of Poincaré map P^n can be visualized using a warp function and animation.

We implemented a set of dynamical systems to demonstrate the usefulness of our techniques. They exhibit most of the characteristics which can be found in 'real world' models. See URL `http://www.cg.tuwien.ac.at/research/vis/dynsys/Poincare97/` for a webpage with images and animations generated during this project. Due to the limited set of advanced visualization techniques in this field, we think that future work on the visualization of Poincaré maps, especially in higher dimensions ($n > 2$) is required.

9 Acknowledgements

The authors would like to thank Helmut Doleisch and Rainer Wegenkittl for helpful comments on preliminary versions of this paper.

References

1. R. H. Abraham and C. D. Shaw. *Dynamics – The Geometry of Behavior.* Addison-Wesley, 2nd edition, 1992.
2. Advanced Visual System Inc. *AVS Developers Guide, Release 4*, May 1992.
3. V. I. Arnold. *Ordinary Differential Equations.* M.I.T. Press, Cambridge, MA, 1973.

4. D. K. Arrowsmith and C. A. Place. *An Introduction to Dynamical Systems.* Cambridge University Press, 1990.
5. Thaddeus Beier and Shawn Neely. Feature-based image metamorphosis. In Edwin E. Catmull, editor, *Computer Graphics (SIGGRAPH '92 Proceedings)*, volume 26, pages 35–42, July 1992.
6. E. Doedel. *Software for Continuation and Bifurcation Problems in Ordinary Differential Equations (AUTO 86 USER MANUAL)*, 2nd edition, February 1986. See also URL `http://ute.usi.utah.edu/software/math/automan.html`.
7. J. H. Hubbard and B. H. West. *Differential Equations: A Dynamical Systems Approach: Ordinary Differential Equations*, volume 5 of *Texts in Applied Mathematics*. Springer, 1991.
8. J. P. M. Hultquist. Constructing stream surfaces in steady 3d vector fields. In *Proceedings Visualization '92*, pages 171–177, October 1992.
9. H. Löffelmann and E. Gröller. DynSys3D: A workbench for developing advanced visualization techniques in the field of three-dimensional dynamical systems. In N. Thalmann and V. Skala, editors, *Proceedings of The Fifth International Conference in Central Europe on Computer Graphics and Visualization '97 (WSCG '97)*, pages 301–310, Plzen, Czech Republic, February 1997.
10. H. Löffelmann, L. Mroz, and E. Gröller. Hierarchical streamarrows for the visualization of dynamical systems. Accepted for publication at the 8th EG Workshop on Visualization in Scientific Computing, Boulogne sur Mer, France, April 1997.
11. H.-O. Peitgen, H. Jürgens, and D. Saupe. *Chaos and Fractals – New Frontiers of Science*. Springer, 1992.
12. H. Poincaré. *Les Méthodes Nouvelles de la Mécanique Céleste (3 vols.).* Gauthier-Villars, Paris, 1899.
13. S. H. Strogatz. *Nonlinear Dynamics and Chaos: with applications to physics, biology, chemistry, and engineering.* Addison-Wesley, 1994.
14. A. A. Tsonis. *Chaos – From Theory to Applications.* Plenum Press, 1992.
15. J. J. van Wijk. Spot noise. In *Proceedings SIGGRAPH '91*, pages 309–318, July 1991.
16. S. Wiggins. *Introduction to Applied Nonlinear Dynamical Systems and Chaos*, volume 2 of *Texts in Applied Mathematics.* Springer, 3rd edition, 1996.

Appendix: example dynamical systems

All the sample systems are 3D flows and exhibit at least one periodic cycle. As a basic example (used for Figs. 1, 6, & 9) we constructed system RealCyc which contains a saddle cycle with a linear Poincaré map, i.e., $P(x) = A \cdot x + b$, that evolves around the z-axis. It is given as follows:

$$\begin{aligned} \dot{x} &= a \cdot x - y \quad \text{with } a = A \cdot (r - 1/r) \ \text{ and } r = \sqrt{x^2 + y^2} \\ \dot{y} &= a \cdot y + x \\ \dot{z} &= C \cdot z \end{aligned}$$

The other sample systems were all together constructed along the same principle: First a 2D system is specified by $\dot{u} = f(u,v)$ and $\dot{v} = g(u,v)$. Functions f and g are modeled such that desired properties are guaranteed (see below). As the next step the 2D system is transformed into half-space $\{(a,b) \,|\, a \geq 0\}$ by transformation $a = e^u$ and $b = v$. Finally the 3D system is constructed by $x = a \cdot \cos\phi$, $y = a \cdot \sin\phi$, and $z = b + h(\phi)$. By differentiation—assuming $\dot{\phi} = \omega$ const.—the 3D flow is derived as follows:

$$\left.\begin{array}{l} \dot{x} = f(u,v)\cdot x - \omega \cdot y \\ \dot{y} = f(u,v)\cdot y + \omega \cdot x \\ \dot{z} = g(u,v) + \omega \cdot \dot{h}(\phi) \end{array}\right\} \text{ with } \left\{\begin{array}{l} u = \ln a \;\text{ and } a = \sqrt{x^2+y^2} \\ v = z - h(\phi) \;\text{ and } x \cdot \tan\phi = y \\ \text{and } \phi \text{ given by } x \cdot \tan\phi = y \end{array}\right.$$

To complete the specifications of NLCyc1, Star, and RTorus, we list functions f, g, and h (assume $h(\phi) \equiv 0$ for all but NLCyc1) that were used for our systems together with a brief explanation of the system parameters:

NLCyc1 – A 3D flow with a non-linear Poincaré map P containing one cycle. Stability characteristics of this cycle depend on A and B. If $C \neq 0$ an oscillation of frequency D is added collinear with the z-axis.

$$\begin{array}{ll} f(u,v) = A \cdot u + (2B - A)\cdot v^2 & \\ g(u,v) = B \cdot v & \text{and } h(\phi) = C \cdot \cos(D \cdot \phi) \end{array}$$

NLCyc1 is visualized in Figs. 2 & 7 .

NLCyc2 – A non-linear saddle cycle, constructed from a linear saddle by applying a rotational shear transformation: $(r,\phi) \rightarrow (r, \phi + D \cdot r)$.

$$\begin{array}{c} \alpha\colon\; u \cdot \tan\alpha = v \;\text{ and } r = \sqrt{u^2+v^2} \;\text{ and } \bar{r} = D \cdot r \\ f(u,v) = (u - \bar{r}\cdot v)\cdot\cos\beta + r \cdot v \cdot \sin\beta \quad \text{with } \beta = 2\cdot(\alpha - \bar{r}) \\ g(u,v) = (v + \bar{r}\cdot u)\cdot\cos\beta - r\cdot u \cdot \sin\beta \end{array}$$

Refer to Fig. 8 for an image of NLCyc2.

RTorus – A 3D flow which exhibits a torus-like invariant set of 'radius' $\sqrt{R}$ within 3D phase space. Its stability characteristics depend on A.

$$\begin{array}{l} f(u,v) = s \cdot u - v \quad \text{with } s = A\cdot(r - R/r) \quad \text{and } r = \sqrt{u^2+v^2} \\ g(u,v) = s \cdot v + u \end{array}$$

RTorus was used for Figs. 4 & 5.

Star – A flow exhibiting a non-hyperbolic saddle cycle, i.e., $\nabla P|_o = 0$. Parameter A controls the number of stable (instable) manifolds. Ω may be used to rotate Poincaré map P around its fixed point $(u,v) = (0,0)$.

$$\begin{array}{c} \alpha\colon\; u \cdot \tan\alpha = v \;\text{ and } r = \sqrt{u^2+v^2} \\ f(u,v) = u \cdot \cos\beta + r \cdot v \cdot \sin\beta \quad \text{with } \beta = A\cdot(\alpha - \Omega) \\ g(u,v) = v \cdot \cos\beta - r \cdot u \cdot \sin\beta \end{array}$$

See Fig. 3 for a visualization of dynamical system Star.

H. Löffelmann, T. Kučera, and E. Gröller: Visualizing Poincaré Maps Together With the Underlying Flow – Color Plates

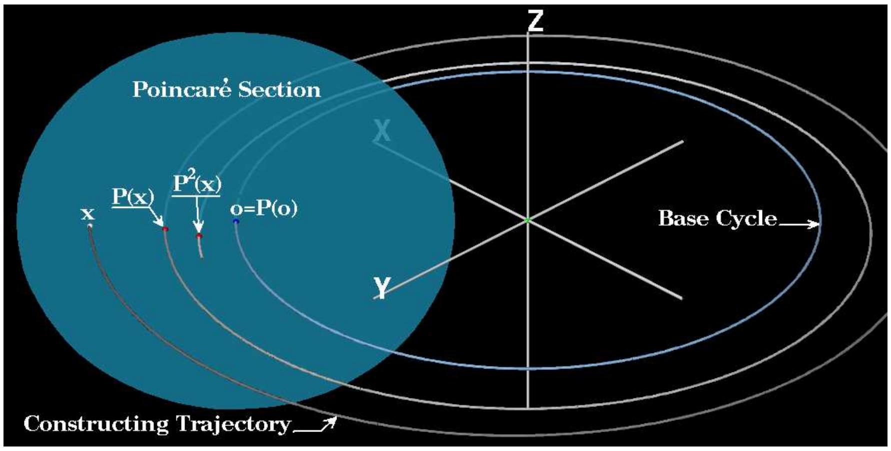

Color Plate 1. An illustration of the Poincaré map definition

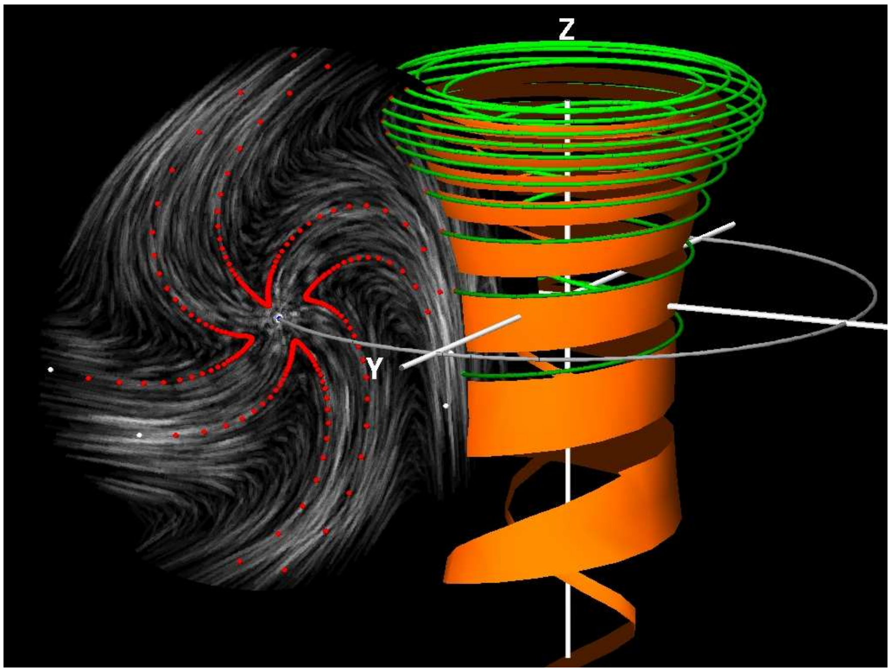

Color Plate 2. Enhancing the 2D Poincaré map visualization by the use of 3D flow visualization icons

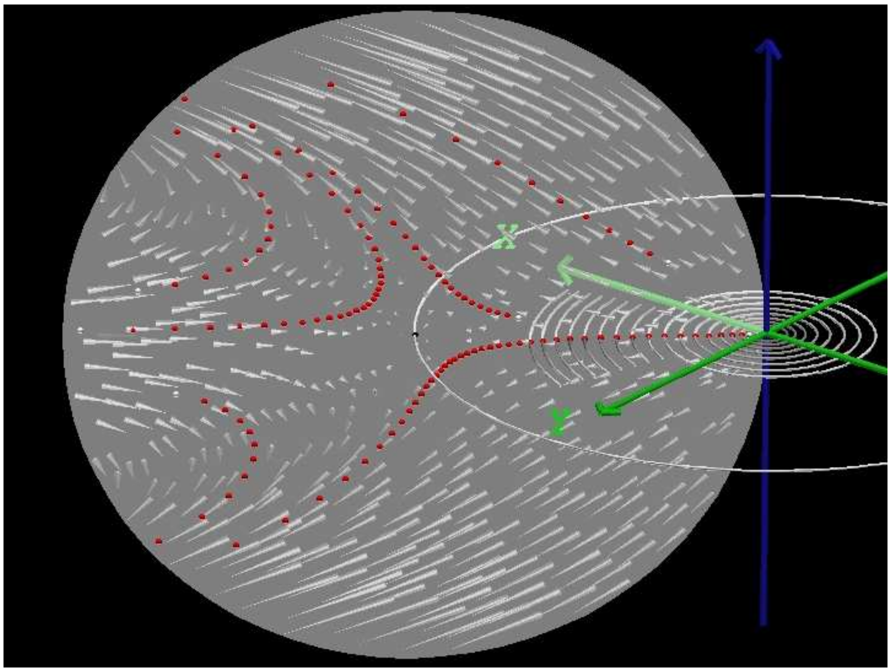

Color Plate 3. Visualizing a non-linear saddle cycle

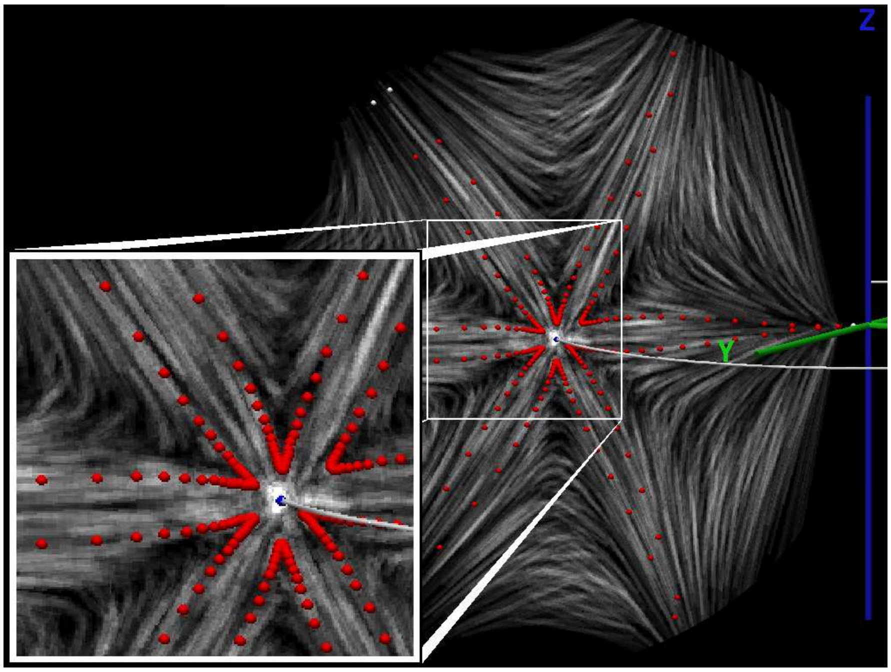

Color Plate 4. Visualizing a non-hyperbolic saddle cycle

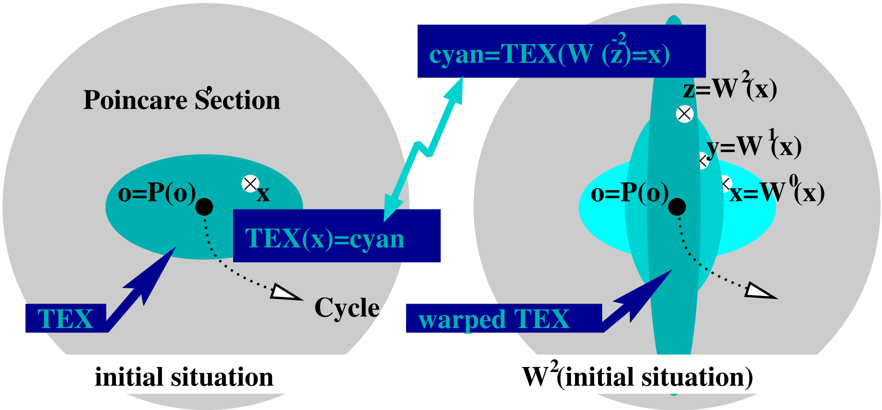

Color Plate 5. Evaluating the initial texture after two applications of W

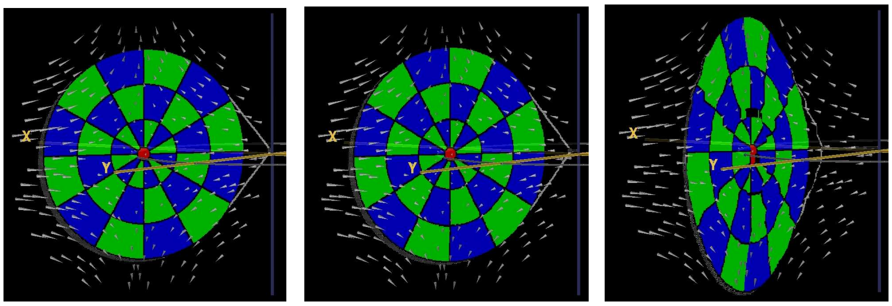

Color Plate 6. Images resulting from one, two, and eleven applications of warp function W, i.e., $W(\mathcal{S})$, $W^2(\mathcal{S})$, and $W^{11}(\mathcal{S})$

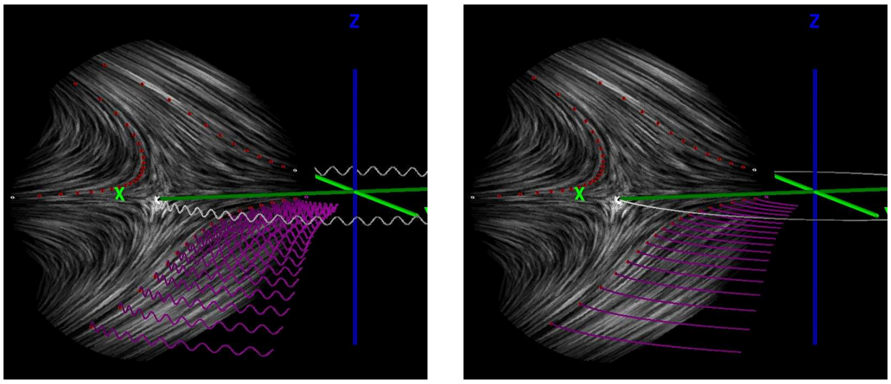

Color Plate 7. Visualizing supplementary information in 3D